Synthesis and Structure of the Group 12 Pyrimidinethiolate Complexes $^{3}_{\infty}$[Zn(S-2-$N_2C_4H_3$)$_2$], $^{2}_{\infty}$[Cd(S-2-$N_2C_4H_3$)$_2$], [Hg(S-2-$N_2C_4H_3$)$_2$] and [Cd(S-2-$N_2C_4H_3$)$_2$(tmeda)]

Andreas Eichhöfer*[a] and Gernot Buth[b]

Keywords: Cadmium / IR spectroscopy / Mercury / N,S ligands / Zinc

The pyrimidinethiolate complexes $^{3}_{\infty}$[Zn(S-2-$N_2C_4H_3$)$_2$], $^{2}_{\infty}$[Cd(S-2-$N_2C_4H_3$)$_2$] and [Hg(S-2-$N_2C_4H_3$)$_2$] have been prepared by reaction of MCl_2 (M = Zn, Cd, Hg) with 2 equiv. of Me_3SiS-2-$N_2C_4H_3$ in organic solvents, whilst [Cd(S-2-$N_2C_4H_3$)$_2$(tmeda)] was obtained by recrystallisation of $^{2}_{\infty}$[Cd(S-2-$N_2C_4H_3$)$_2$] in TMEDA at 40 °C. The structures of the complexes were determined by single-crystal X-ray crystallography, which shows that the different metal atoms each have different coordination environments. The zinc atom in $^{3}_{\infty}$[Zn(S-2-$N_2C_4H_3$)$_2$] exhibits a tetrahedral coordination with one sulfur and three nitrogen atoms from pyrimidinethiolate ligands, whereas the cadmium atoms in $^{2}_{\infty}$[Cd(S-2-$N_2C_4H_3$)$_2$] and [Cd(S-2-$N_2C_4H_3$)$_2$(tmeda)] are six-coordinate with either three sulfur and three nitrogen atoms or two sulfur and four nitrogen atoms. In contrast, the mercury atoms in [Hg(S-2-$N_2C_4H_3$)$_2$] display a distorted square-planar coordination to a pair of chelating $^{-}$S-2-$N_2C_4H_3$ ligands with additional weak Hg–S interactions to adjacent molecules. While known cadmium and zinc pyrimidinethiolate complexes consist of one-dimensional chains, $^{3}_{\infty}$[Zn(S-2-$N_2C_4H_3$)$_2$] and $^{2}_{\infty}$[Cd(S-2-$N_2C_4H_3$)$_2$] form either three- or two-dimensional polymeric networks of metal atoms.

Introduction

There has been considerable interest in the past in the synthesis and coordination properties of chalcogenolates, comprising an amine-based heterocyclic ring, towards group 12 transition metal elements. Heterocyclic thiols, like pyridinethiol or pyrimidinethiol, are some of the most versatile sulfur donor ligands as they can act as monodentate or chelating ligands in the neutral form or as monodentate, chelating and bridging ligands between two or three metal atoms when anionic to yield oligo- or polymeric species.[1,2] Several factors determine the degree of aggregation. [Cd(S-2-NC_5H_4)$_2$][3] and [Zn{S-4,6(CH_3)$_2$-2-N_2C_4H}$_2$],[4] for example, are polymeric, while the additional presence of pyridine in the case of the zinc complex leads to the isolation of the monomeric species [Zn{S-4,6(CH_3)$_2$-2-N_2C_4H}$_2$(NC_5H_5)].[5] Additional bonding of bulky groups near the donor atoms in cadmium complexes leads to a reduction of aggregation, as can be seen in [Cd{S-4,6(CH_3)$_2$-2-N_2C_4H}$_2$]$_6$,[6] which is hexanuclear, and the dimeric [Cd{S-3(CH_3)$_3$Si–NC_5H_4}$_2$]$_2$,[7] which contains the more bulky trimethylsilyl substituent close to the sulfur donor atom. However, [Cd(S-4-CH_3-6-CF_3-2-N_2C_4H)$_2$] is also found to consist of polymeric chains containing octahedrally *cis*-coordinated cadmium atoms.[8] Further influence on the aggregation behaviour also arises from the coordination chemistry of the different metal ions, with mercury preferring lower coordination numbers, as, for example, in [Hg(C_5H_4NS)$_2$][9] and [Hg{S-4,6-(CH_3)$_2$-2-N_2C_4H}$_2$].[10] As well as their rich structural chemistry, additional interest in these ligands also arises from their relationship to pyridine and pyrimidine bases and their nucleosides and nucleotides, which have important roles in living systems, with zinc being bonded to several enzymes and proteins, as well as the search for new antidotes to mercury poisoning.[10] Finally, their also exists a materials aspect to this chemistry as related complexes of cadmium with the general formula [Cd(E-2-NC_5H_6)$_2$]$_n$ (E = S,[11] Se[12]) have been found to be volatile CVD precursors for 12/16 semiconductors.

As a result of our general interest in structural studies of group 12 metal chalcogenide complexes,[13–17] we started studies on the ligand $^{-}$S-4-$N_2C_4H_3$, which has been reported to yield [M(S-2-$N_2C_4H_3$)$_2$] (M = Zn, Cd) in an electrochemical synthesis.[18] However, crystal structures have not been reported to date. Herein, the structures of [M(S-2-$N_2C_4H_3$)$_2$]$_n$ (M = Zn, Cd, Hg) are reported and the complexes synthesised by an organometallic approach.

Results and Discussion

The pyrimidinethiolate complexes $^{3}_{\infty}$[Zn(S-2-$N_2C_4H_3$)$_2$] (**1**), $^{2}_{\infty}$[Cd(S-2-$N_2C_4H_3$)$_2$] (**2**) and [Hg(S-2-$N_2C_4H_3$)$_2$] (**3**)

[a] Institut für Nanotechnologie, Forschungszentrum Karlsruhe, Postfach 3640, 76021 Karlsruhe, Germany
Fax: +49-7247-82-6368
E-mail: eichhoefer@int.fzk.de
[b] Institut für Synchrotronstrahlung, Forschungszentrum Karlsruhe, Postfach 3640, 76021 Karlsruhe, Germany

were prepared as crystalline precipitates by reaction of anhydrous MCl_2 (M = Zn, Cd, Hg) with 2 equiv. of $(CH_3)_3$-SiS-2-$N_2C_4H_3$ in organic solvents according to Scheme 1. Recrystallisation of **2** from TMEDA at room temperature yielded [Cd(S-2-$N_2C_4H_3)_2$(tmeda)] (**4**) nearly quantitatively along with some remaining **2**. Completion of this reaction was achieved by storing the suspension at 40 °C in a dry oven for one week.

MCl_2 + 2 $(CH_3)_3SiS$-2-$N_2C_4H_3$ M = Zn, Cd, Hg

– 2 $ClSiMe_3$ ↓ organic solvent/r.t.

$^3_\infty$[Zn(S-2-$N_2C_4H_3)_2$] (**1**)

$^2_\infty$[Cd(S-2-$N_2C_4H_3)_2$] (**2**)

[Hg(S-2-$N_2C_4H_3)_2$] (**3**)

$^2_\infty$[Cd(S-2-$N_2C_4H_3)_2$] (**2**)

↓ TMEDA/40 °C

[Cd(S-2-$N_2C_4H_3)_2$(tmeda)] (**4**)

Scheme 1.

Complex **1** crystallises in the orthorhombic space group $Pna2_1$. The zinc atoms in **1** are bridged in three dimensions by pyrimidinethiolate ligands to form an infinite network (Figure 1b). A view of a mononuclear fragment is given in Figure 1a, which shows a distorted tetrahedral coordination environment around the zinc atom formed by three nitrogen atoms [N(1), N(3) and N(4)] and one sulfur atom [S(1)]. These atoms belong to two differently coordinating $^-$S-2-$N_2C_4H_3$ ligands in either coordination mode **D** or **E** (Scheme 2). One of them, formed by C(1)–C(4), N(1), N(2) and S(1), bridges a neighbouring zinc atom through the sulfur atom and one nitrogen atom of the ligand, while the additional nitrogen atom N(2) is not involved in further coordination. The other pyrimidinethiolate ligand, consisting of C(5)–C(8), N(3), N(4) and S(2), bridges two adjacent zinc atoms through two of its nitrogen atoms [N(3) and N(4)] whilst the sulfur atom S(2) remains uncoordinated. Neither bridging mode has been observed before in related zinc and cadmium pyrimidinethiolate complexes, which usually comprise a bidentate chelating coordination mode of the ligands towards the metal atoms through a sulfur and a nitrogen atom, as found in [Zn{S-4,6$(CH_3)_2$-2-N_2C_4H}$_2$][4] or [Zn{S-4,6$(CH_3)_2$-2-N_2C_4H}$_2$$(NC_5H_5)$].[5] However, the Zn–N (205.3–209.8 pm) and Zn–S (234.4 pm) bond lengths in **1** are comparable to the related distances observed in theses complexes. The three-dimensional network in **1** is formed by helical chains of alternating zinc atoms and pyrimidinethiolate ligands in bridging mode **D** arranged along the crystallographic *c*-axis (2_1 symmetry) which are themselves further crosslinked through $^-$S-2-$N_2C_4H_3$ ligands in the coordination mode **E** (Figure 1b). This differs from known structures formed by pyrimidine- and pyridinethiolates with group 12 transition elements, such as [Cd(S-2-$NC_5H_4)_2$],[3] [Zn{S-4,6$(CH_3)_2$-2-N_2C_4H}$_2$],[4] [Cd(S-4-CH_3-6-CF_3-2-$N_2C_4H)_2$][8] and [$Hg(C_5H_4NS)_2$],[9] which all consist of chain structures.

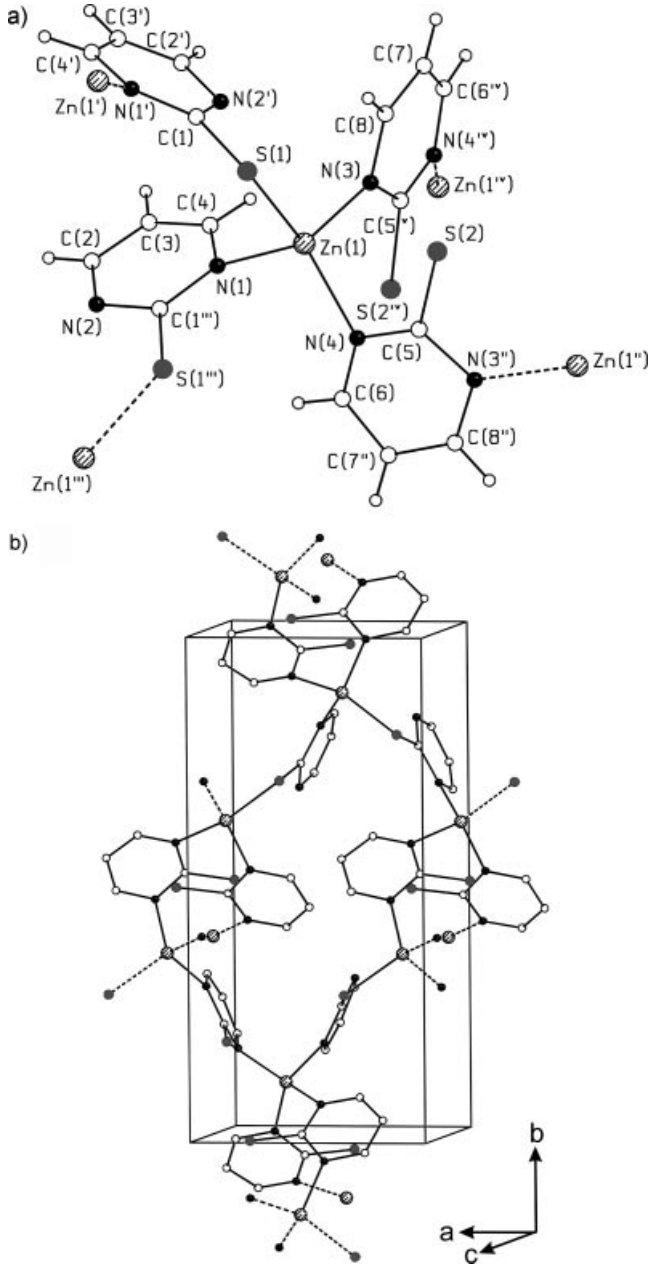

Figure 1. a) View of the coordination sphere of the zinc atom in [Zn(S-2-$N_2C_4H_3)_2$] (**1**). b) Section of the three-dimensional polymeric network in **1**. Symmetry transformation for generation of equivalent atoms [I]: $x + 1/2, -y + 3/2, z$; [II]: $-x, -y + 1, z + 1/2$; [III]: $x - 1/2, -y + 3/2, z$; [IV]: $-x, -y + 1, z - 1/2$. Selected bond lengths [pm] and angles [°]: Zn(1)–N(4) 205.3 (10), Zn(1)–N(3) 206.5(11), Zn(1)–N(1) 209.8(12), Zn(1)–S(1) 234.4(4); N(4)–Zn(1)–N(3) 106.1(4), N(4)–Zn(1)–N(1) 107.0(4), N(3)–Zn(1)–N(1) 104.7(4), N(4)–Zn(1)–S(1) 127.2(3), N(3)–Zn(1)–S(1) 109.1(3), N(1)–Zn(1)–S(1) 100.7(3).

Complex **2** crystallises in the orthorhombic space group *Pbca*. Figure 2 shows a view of the coordination sphere of the cadmium atom (Cd1) in **2**, which is six-coordinate with

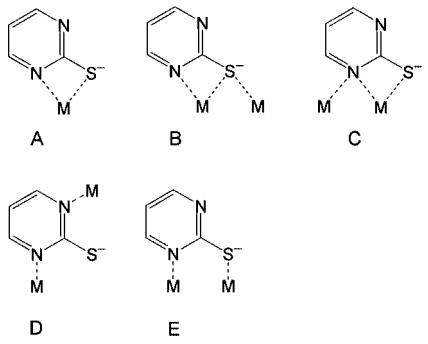

Scheme 2. Schematic drawing of the coordination modes of the pyrimidinethiolate ligand ($^{-}$S-2-$N_2C_4H_3$) found in **1**–**4**.

three sulfur [S(1), S(2) and S(2′)] and three nitrogen atoms [N(1)–N(3)]. Two pairs of sulfur and nitrogen atoms [S(2′), N(3) and S(1), N(1)] belong to two $^{-}$S-2-$N_2C_4H_3$ ligands that chelate the cadmium atom with bite angles of 59° and 61.6(1)° for N(3)–Cd(1)–S(2′) and N(1)–Cd(1)–S(1), respectively. These values are comparable to those found in the monomeric complex [Cd(S-2-$N_2C_4H_3)_2$(phen)].[18] However, further coordination of each of the pyrimidine-2-thiolate ligands is different, with one of the ligands coordinating additionally through the sulfur atom [S(2′)] to a neighbouring cadmium atom [Cd(1′)] to form an asymmetric μ_2-S-2-$N_2C_4H_3$ bridge and the other additionally binding through the free nitrogen atom [N(2′′)] to another neighbouring cadmium atom [Cd(1′′)]. Whilst the Cd–S bond of the pure chelating μ_2-S-2-$N_2C_4H_3$ ligand [Cd(1)–S(1): 261.2(2)] is comparable to that found in the monomeric complex [Cd(S-2-$N_2C_4H_3)_2$(phen)], the Cd–S bonds of the other pyrimidine-2-thiolate ligand, which acts as both a bidentate and a μ_2-bridging ligand, exhibit one shorter [Cd(1)–S(2): 260.3(2) pm] and one longer distance [Cd(1)–S(2′) 292.6(2) pm]. This effect of a weakening of the Cd–S chelating bond upon formation of additional μ_2-bridges has also been observed to a different extent in other complexes that contain heterocyclic thiolates as ligands, such as [Cd(S-2-$NC_5H_4)_2$],[3] [Cd{S-4,6-$(CH_3)_2$-2-N_2C_4H}$_2$]$_6$,[6] [Cd{S-3-$(CH_3)_3SiNC_5H_4$}$_2$]$_2$[7] and [Cd(S-4-CH_3-6-CF_3-2-$N_2C_4H)_2$].[8] The Cd–N bond lengths, which range from 233.3(5) to 248.0(6) pm, are also comparable to those found for the six-coordinate cadmium complexes mentioned above. In the crystal structure (Figure 2b), each cadmium atom is therefore linked to a total of three other cadmium atoms. One connection consists of two μ_2-S-2-$N_2C_4H_3$ bridges, each of which additionally chelates one of the two cadmium atoms, and the other two linkages are each formed by a single $^{-}$S-2-$N_2C_4H_3$ ligand in two inverted coordination forms. In one case the ligand chelates the central cadmium atom and acts as a monodentate ligand through the other nitrogen atom towards the neighbouring metal atom and in the other case the other way round. In this way **2** forms a distorted two-dimensional honeycomb network in the 011 plane which is in contrast to related structures in the literature which consist of one-dimensional polymeric structures.

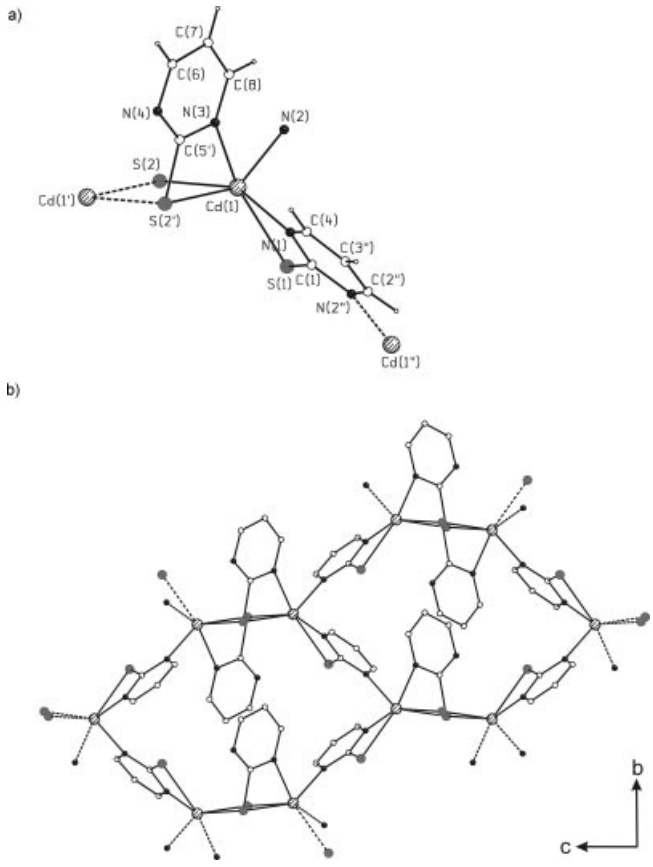

Figure 2. a) View of the coordination sphere of the cadmium atoms in [Cd(S-2-$N_2C_4H_3)_2$] (**2**). b) Section of the two-dimensional polymeric network in **2** viewed along *a*. Symmetry transformation for generation of equivalent atoms ^{I}: $-x$, $-y$, $-z + 1$; ^{II}: $-x$, $y + 1/2$, $-z + 3/2$; ^{III}: $-x$, $y - 1/2$, $-z + 3/2$. Selected bond lengths [pm] and angles [°]: Cd(1)–N(1) 248.0(6), Cd(1)–N(2) 240.2(5), Cd(1)–N(3) 233.3(5), Cd(1)–S(1) 261.2(2), Cd(1)–S(2) 260.3(2), Cd(1)–S(2′ 292.7(2); N(3)–Cd(1)–N(2) 90.4(2), N(3)–Cd(1)–N(1) 95.3(2), N(2)–Cd(1)–N(1) 113.3(2), N(3)–Cd(1)–S(2) 96.5(2), N(2)–Cd(1)–S(2) 91.9(1), N(1)–Cd(1)–S(2) 152.1(1), N(3)–Cd(1)–S(1) 156.5(1), N(2)–Cd(1)–S(1) 95.0(1), N(1)–Cd(1)–S(1) 61.6(1), S(2)–Cd(1)–S(1) 106.1(1), N(3)–Cd(1)–S(2)′ 59.0(1), N(2)–Cd(1)–S(2)′ 148.5(1), N(1)–Cd(1)–S(2)′ 79.4(1), S(2)–Cd(1)–S(2)′ 85.3(1), S(1)–Cd(1)–S(2)′ 115.9(1).

Complex **3** crystallises in the monoclinic space group $P2_1/n$ with two independent molecules **3a** and **3b**, which differ slightly in their geometry, in the asymmetric unit (Figure 3). In both molecules the mercury atoms are four-coordinate and are chelated by two $^{-}$S-2-$N_2C_4H_3$ ligands in a bidentate fashion through the sulfur atom and one nitrogen atom, with S–Hg–N bite angles ranging from 59.65° to 61.35° (coordination mode **A** in Scheme 2). Molecule **3a** [Hg(2), S(3), S(4), N(5)–N(8), C(9)–C(16)] (Figure 3a) exhibits an almost square-planar coordination of the mercury atom with a maximum deviation of 0.151(4) pm for S(4) from the molecular plane and a torsion angle along C(9)–S(3)–S(4)–C(13) of 176.9°. In molecule **3b** [Hg(1), S(1), S(2), N(1)–N(4), C(1)–C(8); (Figure 3b)], the pyrimidinethiolate ligands are twisted from this plane to give a torsion angle of 151.9° along C(1)–S(1)–S(2)–C(5). Mean Hg–S bond lengths of around 235.4 pm as well as mean Hg–N separa-

tions around 287.9 pm are comparable to those found in similar compounds like $[Hg(C_5H_4NS)_2]$[9] and $[Hg\{S\text{-}4,6\text{-}(CH_3)_2\text{-}2\text{-}N_2C_4H\}_2]$.[10] Additional weaker Hg–S separations with a mean value of 329.9 pm lead to the formation of one-dimensional chains for both forms of **3a** and **3b** (shown only for **3b** in Figure 3b). While the mercury thiopyridine structure also contains mercury(II) ions in a square-planar environment with a similar chain structure, the pyrimidinethiolate derivative exhibits five-coordinate metal atoms, which leads in the crystal structure to the formation of a helix-like polymer chain of the molecular units.

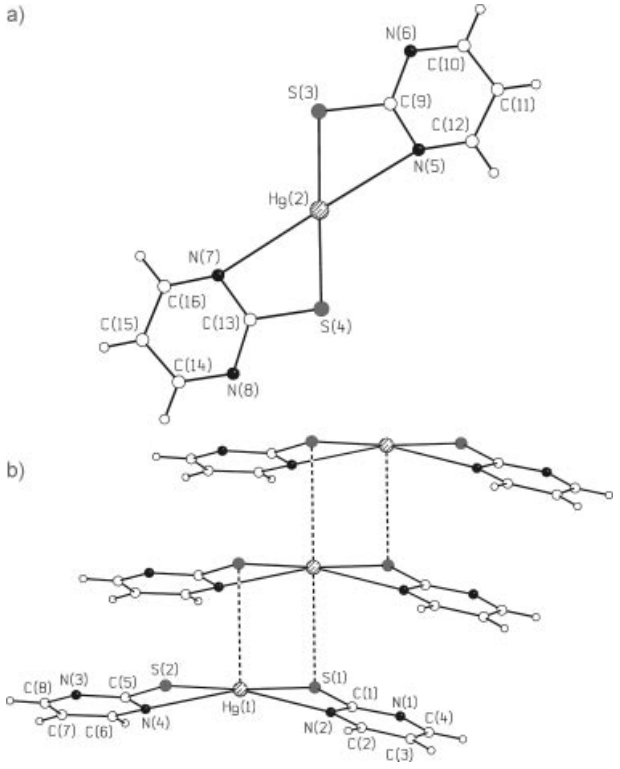

Figure 3. Molecular structures of the two independent molecules in $[Hg(S\text{-}2\text{-}N_2C_4H_3)_2]$ (**3a**/**3b**) with a drawing of the chain structure formed by weak intermolecular Hg–S interactions (dotted lines). Selected bond lengths [pm] and angles [°]: Hg(1)–S(2) 235.0(2), Hg(1)–S(1) 236.0(2), Hg(1)–N(4) 290.7(7), Hg(1)–N(2) 281.5(6), Hg(2)–S(4) 234.9(2), Hg(2)–S(3) 235.5(2), Hg(2)–N(5) 286.0(6), Hg(2)–N(7) 293.5(6); S(2)–Hg(1)–S(1) 176.06(7), S(1)–Hg(1)–N(2) 61.4(1), S(2)–Hg(1)–N(4) 60.1(1), N(4)–Hg(1)–N(2) 157.1(1), S(4)–Hg(2)–S(3) 178.7(1), S(4)–Hg(2)–N(7) 59.7(1), S(3)–Hg(2)–N(5) 60.8(1), N(5)–Hg(2)–N(7) 177.3(1). Weak intermolecular Hg–S interactions [pm]: Hg(1)···S(1) 322.9, Hg(1)···S(2) 338.8, Hg(2)···S(3) 331.1, Hg(2)···S(4) 326.7.

Monomeric **4** crystallises in the monoclinic space group $P2_1/n$ (Figure 4) and exhibits a highly distorted octahedral coordination around the cadmium atom. The coordination sphere involves two nitrogen atoms [N(5) and N(6)] from the bidentate TMEDA ligand, and one sulfur atom [S(1) and S(2)] and one nitrogen atom [N(1) and N(3)] belonging to each of two pyrimidine-2-thiolate ligands. The bond lengths and bite angles of the three bidentate ligands are similar to those found in $[Cd(S\text{-}2\text{-}N_2C_4H_3)_2(phen)]$[18] and **2** as discussed above.

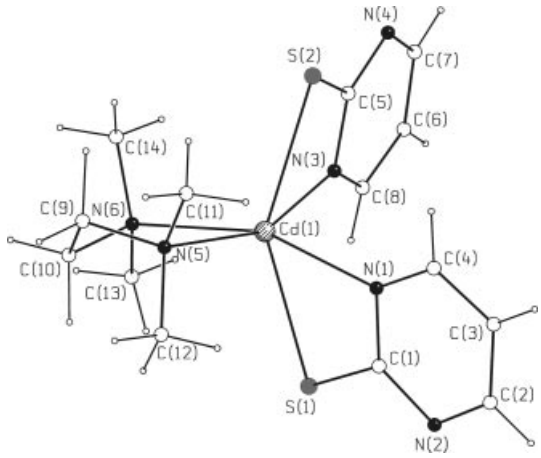

Figure 4. Molecular structure of $[Cd(S\text{-}2\text{-}N_2C_4H_3)_2(tmeda)]$ (**4**). Selected bond lengths [pm] and angles [°]: Cd(1)–N(6) 240.0(2), Cd(1)–N(5) 240.4(2), Cd(1)–N(1) 244.0(2), Cd(1)–N(3) 245.1(2), Cd(1)–S(1) 260.7(1), Cd(1)–S(2) 260.9(1); N(6)–Cd(1)–N(5) 76.1(1), N(6)–Cd(1)–N(1) 158.6(1), N(5)–Cd(1)–N(1) 91.5(1), N(6)–Cd(1)–N(3) 90.4(1), N(5)–Cd(1)–N(3) 158.9(1), N(1)–Cd(1)–N(3) 106.0(1), N(6)–Cd(1)–S(1) 102.3(1), N(5)–Cd(1)–S(1) 101.3(1), N(1)–Cd(1)–S(1) 62.7(1), N(3)–Cd(1)–S(1) 97.4(1), N(6)–Cd(1)–S(2) 103.7(1), N(5)–Cd(1)–S(2) 104.7(1), N(1)–Cd(1)–S(2) 96.2(1), N(3)–Cd(1)–S(2) 62.3(1), S(1)–Cd(1)–S(2) 146.8(1).

A comparison of the powder diffraction patterns of the crystalline precipitates of **1**–**4** with the calculated pattern of the crystals investigated by single-crystal X-ray analysis displays a good agreement, which proves, together with the elemental analysis, the purity of the compounds (Figure 5). Small deviations in intensity and reflection position at higher angles might be due to the fact that the powder measurements were done at room temperature in contrast to 190 K for the single-crystal measurement, and that needle-like crystals (e.g. **3**) preferably align in the capillary vertical to the beam.

The IR spectra of **1**–**3** (Figure 6) differ from that of the neutral thiol $HS\text{-}2\text{-}N_2C_4H_3$, in agreement with coordination of the monoanion $^-S\text{-}2\text{-}N_2C_4H_3$ to the metal atoms. Additionally, there are differences between the spectra of **1**–**3** due to the different coordination modes of the pyrimidinethiolate ligand towards the metal atoms. As IR data for complexes of monoanionic pyridine- and pyrimidinethiolate ligands are rare and have not been assigned in full detail, the discussion mostly refers to the spectra of the neutral thiol $HS\text{-}2\text{-}N_2C_4H_3$[19,20] and a study of several metal complexes of pyridinethiol.[21] In solution, pyrimidines and pyridines that are substituted at the 2- or 4-position by thiol groups can exist in two tautomeric forms **I** (thiol) and **II** (thione; Scheme 3).[22] In the solid state, 2-mercaptopyridine and 4-mercaptopyridine have been found to exist as H-bonded dimers of the thione form.[23,24] Similarly, it might be assumed that 2-mercaptopyrimidine also exists in the solid state as an H-bonded dimer, displayed in Scheme 3 as form **III**. Evidence for this in the IR spectrum of $HS\text{-}2\text{-}N_2C_4H_3$ is a broad band around 2633 cm^{-1}, which can be assigned to the stretching of the N–H bonds being strongly hydrogen-bonded in the solid state, and the three bands

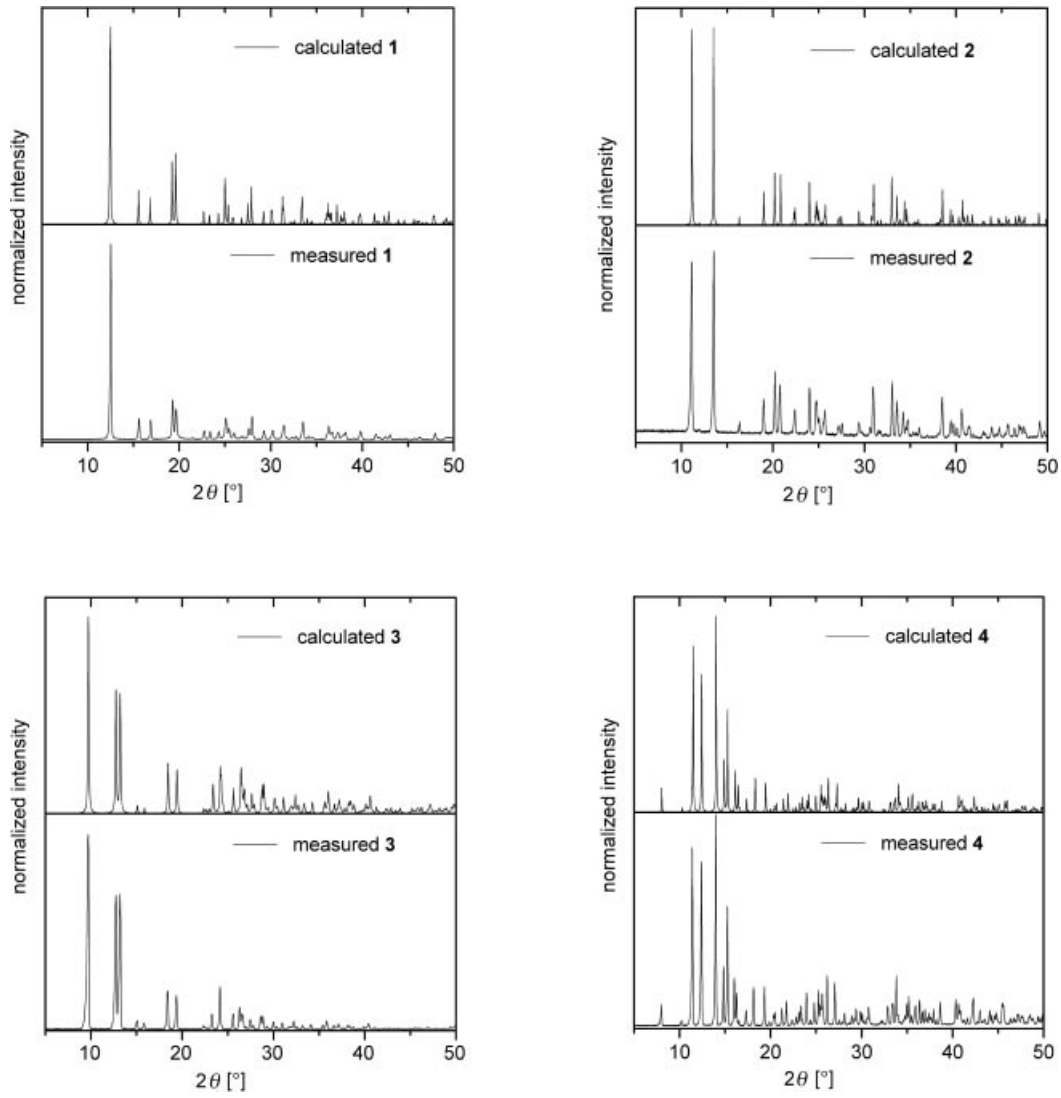

Figure 5. Calculated (top) and measured (bottom) powder XRD pattern of $[Zn(S\text{-}2\text{-}N_2C_4H_3)_2]$ (**1**), $[Cd(S\text{-}2\text{-}N_2C_4H_3)_2]$ (**2**), $[Hg(S\text{-}2\text{-}N_2C_4H_3)_2]$ (**3**) and $[Cd(S\text{-}2\text{-}N_2C_4H_3)_2(tmeda)]$ (**4**).

near 2000 cm^{-1}, which can be assigned as a result of Fermi resonances and overtones of the ν(N–H) mode. Both these features are absent from the IR spectra of **1**–**3** because of the anionic character of the ligand. However, one can see the peaks that result from the C–H stretching vibrations of the aromatic pyrimidine rings between 3100 and 3000 cm^{-1}. The aromatic ring stretching vibrations (C=C and C=N), which fall in the region from 1600 to 1500 cm^{-1}, show a characteristic two-band structure with slightly shifted peak positions in **1**–**3**, especially when compared to the ligand spectrum. In the region further down to 1250 cm^{-1}, a strong and broad peak around 1370 cm^{-1}, which probably consists of several vibrations, is visible in all three group 12 metal pyrimidinethiolates rather than the three separate peaks at 1492, 1424 and 1333 cm^{-1} in the free thiol, which are assigned to ring stretching and C–H bending vibrations. This is followed by a pair of strong peaks (three peaks for **1**) at around 1200 cm^{-1}. These bands are interpreted as being due to C–H bending and C–S stretching vibrations in the neutral ligand. Interestingly, Kennedy et al. have found that extensive coupling within the ring system, as indicated, for example, by an ^{18}O study of 2-hydroxypyridine,[25] precludes the identification of any band definitively assigned to a C–S stretching vibration.[21] Two peaks in the spectrum of pyrimidinethiol at 1051 and 983 cm^{-1} have been assigned as ring breathing vibrations.[20] These are significantly altered in the spectra of the three metal complexes **1**–**3** of the anionic pyrimidine-2-thiolate ligand. A shift in the ring breathing mode in simple pyridine–metal complexes is used as a guide to metal coordination.[26] However, for metal complexes of 2-pyridinethiol and 4-pyridinethiol it has been found that changes in energy of these bands are indicative of a change in coordination but not informative concerning the mode of the coordination.[21] Further down, the neutral ligand displays two peaks at 793 and 751(sh) cm^{-1}, characteristic of a mono-substituted aromatic ring, which have been assigned to C–H bending and a combination of C–S stretching, C–H bending and ring deformation modes,

respectively. While one observes a similar group in **1**, consisting of a single peak at 810 cm^{-1} and a second peak at 750 cm^{-1} with a shoulder at 768 cm^{-1}, this second peak splits in **2** and **3** to give two well-separated peaks at either 767 and 746 cm^{-1} or 769 and 743 cm^{-1}, respectively. Four more peaks can be identified down to 300 cm^{-1} for HS-2-$N_2C_4H_3$, which are assigned to either ring deformation (625 cm^{-1}) and/or C–S bending and stretching modes (486, 472 cm^{-1} and 406 cm^{-1}). This area displays the most visible changes in the IR spectra for **1**–**3**, indicative of the different coordination modes of the anionic pyrimidinethiolate ligand towards the metal atoms. New bands arise in the spectra of **1**–**3** compared to the neutral ligand in the far-IR region below 300 cm^{-1}. For complexes of the type $[MX_2L_2]$ (M = Zn, Cd, Hg; X = Cl, Br and L = Py-2-SH, Py-4-SH), bands between 198 and 235 cm^{-1} have been assigned as M–L vibrational modes.[21] In pyridine complexes like $[Zn(py)_2X_2]$, M–Py vibrations have been assigned by the isotope technique in the region of 200 to 225 cm^{-1}.[27,26] Interestingly, **3** displays only one strong peak in this region at 254 cm^{-1}, probably due to the symmetric square-planar coordination environment of the metal atom, while the spectra of **1** and **2** contain several peaks.

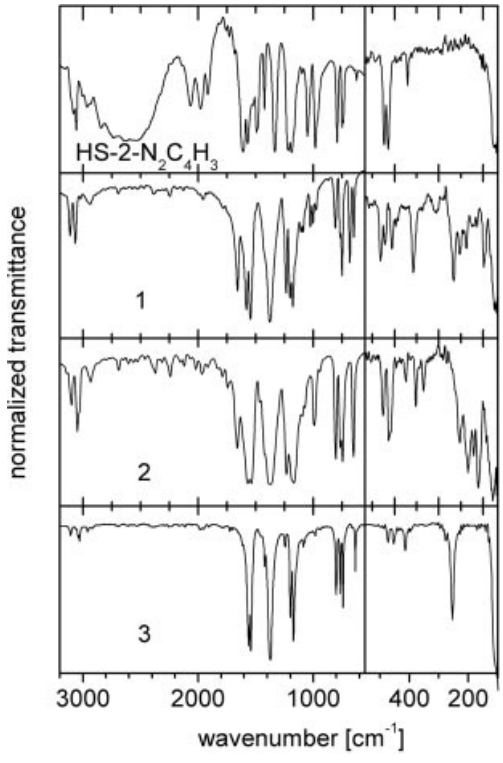

Figure 6. Comparison of the IR spectra of HS-2-$N_2C_4H_3$ (top), $[Zn(S\text{-}2\text{-}N_2C_4H_3)_2]$ (**1**), $[Cd(S\text{-}2\text{-}N_2C_4H_3)_2]$ (**2**) and $[Hg(S\text{-}2\text{-}N_2C_4H_3)_2]$ (**3**) measured as a CsI pellets.

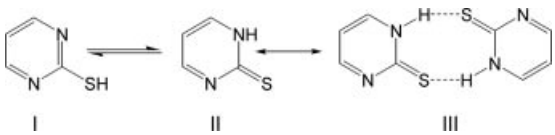

Scheme 3.

The UV/Vis spectra in the solid state display a shift in the absorption onset on going from **1** (450 nm) to **2** (430 nm) to **4** (395 nm) to **3** (366 nm) in such a way that the zinc complex **1** absorbs at higher wavelengths (lower energy) than the other complexes **2**, **3**, **4**. Apart from the spectrum of **1**, which shows a shoulder at 375 nm followed by a broad peak at 285 nm, and **4**, which displays a shoulder at 325 nm followed by a peak at 285 nm, the spectra of **1**–**4** are almost featureless.

The ^1H and ^{13}C NMR spectra of the complexes in dimethyl sulfoxide display similar peak patterns for the pyrimidinethiolate ligand to those observed for the precursor compound $(CH_3)_3S\text{-}2\text{-}N_2C_4H_3$, with only slightly shifted positions of the signals. In contrast to the situation found in the crystalline state, the equivalence of the two hydrogen and carbon atoms in the *meta* position indicates a symmetric coordination of the ligand in solution that is probably generated by a complex equilibrium with fast exchange between different coordination modes.

Experimental Section

Physical Measurements: ^1H and ^{13}C NMR spectra were recorded with a Bruker DPX Avance 300. ^{29}Si NMR spectra were measured with a Bruker Avance 400. UV/Vis absorption spectra of cluster molecules in solution were measured with a Varian Cary 500 spectrophotometer in quartz cuvettes. Solid-state reflection spectra were measured as micron-sized crystalline powders between quartz plates with a Labsphere integrating sphere. IR and FIR spectra were measured with a Perkin–Elmer Spectrum GX as CsI pellets in the region from 4000 to 30 cm^{-1}.

Synthesis: Standard Schlenk techniques were employed throughout the syntheses using a double-manifold vacuum line with high-purity dry nitrogen. The solvent diethyl ether was dried with sodium/benzophenone and distilled under nitrogen. Anhydrous DMF ($H_2O < 0.005\%$) and pyridine ($H_2O < 0.01$) obtained from Aldrich were degassed, freshly distilled and stored over molecular sieves under nitrogen. Anhydrous $ZnCl_2$, $CdCl_2$ and $HgCl_2$ were purchased from Aldrich. $(2\text{-}N_2C_4H_3)SSiMe_3$ was prepared according to a general procedure for silylthiopyrimidines.[28] Thus, $(2\text{-}N_2C_4H_3)SH$ [6 g (0.0535 mol)] was dissolved in a mixture of 130 mL of hexamethyldisilazane (HDMS) and 50 mL of dioxane and heated under reflux for 24 h. Excess HDMS and dioxane were removed by distillation and the remaining oil distilled under vacuum (1×10^{-3} mbar) to yield $(2\text{-}N_2C_4H_3)SSiMe_3$ as a yellow oily liquid (b.p. 70 °C). Yield: 8.93 g (90.6%). ^1H NMR (300 MHz, C_6D_6): $\delta = 0.52$ [s, $Si(CH_3)_3$, 9 H], 6.54 (t, $^3J_{H,H} = 4.9$ Hz, *para*-C*H*, 1 H), 8.18 (d, $^3J_{H,H} = 4.9$ Hz, *meta*-C*H*, 2 H) ppm. $^{13}C\{^1H\}$NMR (75 MHz, C_6D_6): $\delta = 1.4$ [s, $Si(CH_3)_3$], 117.1 (s, *meta*-*C*H), 157.3 (s, *para*-*C*H), 172.9 (s, *C*SSi) ppm. ^{29}Si NMR (79.5 MHz, C_6D_6): $\delta = 15.7$ [s, $Si(CH_3)_3$] ppm.

$[Zn(S\text{-}2\text{-}N_2C_4H_3)_2]$ (1): $ZnCl_2$ (0.14 g, 1.03 mmol) was dissolved in 20 mL of DMF. $(2\text{-}N_2C_4H_3)SSiMe_3$ (0.4 mL, 2.18 mmol) was then added at 0 °C and the resulting yellow solution slowly warmed to room temperature. After a short time, **1** started to precipitate as a pale-yellow crystalline powder. The crystallisation was completed by layering the reaction solution with diethyl ether by evaporation and condensation from a connected flask. Yield: 0.25 g (84.5%). $C_8H_6N_4S_2Zn$ (287.7): calcd. C 33.4, H 2.1, N 19.5, S 22.3; found C 33.5, H 2.4, N 19.5, S 21.5. Small but suitable crystals for single-

crystal X-ray analysis were found in carefully layered DMF solutions of **1** with diethyl ether or directly in carefully warmed up reaction solutions. IR (CsI): $\tilde{\nu}$ = 3111 (m), 3066 (m), 3021 (w), 2940 (w, br), 2693 (w), 2389 (w), 2245 (w), 1956 (w, br), 1782 (w), 1657 (s), 1580 (vs), 1545 (vs), 1377 (vs, br), 1235 (s), 1202 (vs), 1178 (vs), 1106 (m), 1088 (m), 1025 (m), 1001 (m), 976 (w), 810 (m), 750 (s, sh), 684 (s), 648 (m), 498 (m), 483 (m), 459 (m), 446 (w), 386 (m), 250 (m), 230 (m), 207 (m), 187 (w, sh), 170 (w), 148 (m) cm^{-1}. UV/Vis (nujol): λ_{max} = 375 (sh), 285 (vbr) nm. ^1H NMR (300 MHz, $(CD_3)_2SO$]: δ = 6.9 (t, $^3J_{H,H}$ = 4.9 Hz, *para*-C*H*, 1 H), 8.3 (d, $^3J_{H,H}$ = 4.9 Hz, *meta*-C*H*, 2 H) ppm. $^{13}C\{^1H\}$ NMR [75 MHz, $(CD_3)_2SO$]: δ = 114.9 (s, *meta*-*C*H), 157.6 (s, *para*-*C*H), 182.6 (s, *C*SSi) ppm.

[Cd(S-2-$N_2C_4H_3$)$_2$] (2): $CdCl_2$ (0.4 g, 2.18 mmol) was dissolved in 55 mL of DMF. (2-$N_2C_4H_3$)$SSiMe_3$ (0.8 mL, 4.36 mmol) was then added at 0 °C and the resulting yellow solution warmed to room temperature. After a short time, **2** precipitated as a white crystalline powder. Yield: 0.53 g (73%). $C_8H_6CdN_4S_2$ (334.7): calcd. C 28.7, H 1.8, N 16.7, S 19.2; found C 28.8, H 1.9, N 16.1, S 19.2. Crystals suitable for single-crystal X-ray analysis were grown upon layering DMF/pyridine (1:1) solutions of **2** with diethyl ether. IR (CsI): $\tilde{\nu}$ = 3098 (m), 3048 (s), 2932 (w), 2688 (w), 2371 (w, sh), 2242 (w, sh), 1966 (w, b), 1789 (w), 1744 (w), 1659 (s), 1569 (vs), 1540 (vs), 1373 (vs, b), 1232 (vs), 1169 (vs, sh), 994 (s), 806 (s), 765 (s), 746 (s), 652(s), 488 (m), 465 (s), 412 (w), 378 (m), 352 (w), 229 (s), 201 (s), 182 (s), 167 (s) cm^{-1}. UV/Vis (nujol): λ_{max} = 350 (sh), 292 (vbr) nm. ^1H NMR (300 MHz, $(CD_3)_2SO$]: δ = 6.9 (t, $^3J_{H,H}$ = 4.9 Hz, *para*-C*H*, 1 H), 8.2 (d, $^3J_{H,H}$ = 4.9 Hz, *meta*-C*H*, 2 H) ppm. $^{13}C\{^1H\}$ NMR [75 MHz, $(CD_3)_2SO$]: δ = 114.6 (s, *meta*-*C*H), 157.3 (s, *para*-*C*H), 183.5 (s, *C*SSi) ppm.

[Hg(S-2-$N_2C_4H_3$)$_2$] (3): $HgCl_2$ (0.21 g, 0.78 mmol) was dissolved in 25 mL of acetonitrile. (2-$N_2C_4H_3$)$SSiMe_3$ (0.3 mL, 1.62 mmol) was then added at 0 °C which resulted immediately in the formation of a white and fluffy precipitate of **3**. After warming up to room temperature, **3** was filtered and washed twice with diethyl ether. Yield: 0.3 g (90.9%). $C_8H_6HgN_4S_2$ (422.9): calcd. C 22.7, H 1.4, N 13.3, S 15.2; found C 23.2, H 1.5, N 13.7, S 15.4. Crystals suitable for single-crystal X-ray analysis were grown by recrystallisation of ca. 30 mg of **3** from 10 mL of hot CH_3CN/DMF (10:2). IR (CsI): $\tilde{\nu}$ = 3108 (w), 3029 (w,sh), 2959 (w), 1726 (w), 1704 (w), 1560 (vs), 1542 (vs), 1423 (m), 1372 (vs), 1242 (w, sh), 1200 (s), 1173 (vs), 1087 (w, sh), 983 (w, sh), 803 (m), 769 (m), 743 (s), 635 (m), 473 (w), 454 (w), 414 (w), 279 (w), 254 (s) cm^{-1}. UV/Vis (nujol): λ_{max} = 280 (vbr) nm. ^1H NMR [300 MHz, $(CD_3)_2SO$]: δ = 7.2 (t, $^3J_{H,H}$ = 4.9 Hz, *para*-C*H*, 1 H), 8.5 (d, $^3J_{H,H}$ = 4.9 Hz, *meta*-C*H*, 2 H) ppm. $^{13}C\{^1H\}$ NMR [75 MHz, $(CD_3)_2SO$]: δ = 117.7 (s, *meta*-*C*H), 158.3 (s, *para*-*C*H), 176.5 (s, *C*SSi) ppm.

[Cd(S-2-$N_2C_4H_3$)$_2$(tmeda)] (4): Complex **1** (0.05 g, 0.15 mmol) was suspended in 15 mL of TMEDA for 2 min in an ultrasonic bath. Then, the flask was sealed with a Teflon screw tap and placed in a dry oven at 35 °C for one week to yield **4** as a white crystalline powder. Yield: 0.066 g (98%). $C_{14}H_{22}CdN_6S_2$ (450.9): calcd. C 37.3, H 4.9, N 18.6, S 14.2; found C 37.1, H 4.9, N 19.4, S 14.6. Crystals suitable for single-crystal X-ray analysis were grown by allowing the solution to stand at room temperature. IR (CsI): $\tilde{\nu}$ = 3097 (w), 3044 (w, sh), 2980 (m), 2956 (m), 2874 (m, br), 2847 (m), 2800 (m), 1730 (w), 1538 (vs), 1569 (vs), 1463 (s), 1426 (s), 1372 (vs), 1298 (m), 1239 (s), 1211 (s), 1181 (vs), 1134 (w), 1103 (w), 1068 (m), 1036 (m), 1019 (m), 983 (m), 953 (s), 791 (s, sh), 770 (s), 744 (s), 646 (m), 584 (w), 485 (m), 462 (s), 447 (w, sh), 433 (m), 401 (w), 377 (w, sh), 244 (w), 203 (s, sh), 181 (m, br), 171 (w, sh), 152 (m, sh), 142 (w), 135 (w) cm^{-1}. UV/Vis (nujol): λ_{max} = 325 (sh) 285 (br) nm. ^1H NMR [300 MHz, $(CD_3)_2SO$]: δ = 2.3 (s, N*C*H_3, 12 H), 2.5 (s, *C*H_2N, 4 H), 6.9 (t, $^3J_{H,H}$ = 4.9 Hz, *para*-C*H*, 1 H), 8.3 (d, $^3J_{H,H}$ = 4.9 Hz, *meta*-C*H*, 2 H) ppm. $^{13}C\{^1H\}$ NMR [75 MHz, $(CD_3)_2SO$]: δ = 47.0 (s, N*C*H_3), 57.1 (s, *C*H_2N), 114.8 (s, *meta*-*C*H), 157.5 (s, *para*-*C*H), 183.5 (s, *C*SSi) ppm.

Crystallography: Crystals suitable for single-crystal X-ray diffraction were taken directly from the reaction solution of the compound and then selected in perfluoroalkylether oil. Single-crystal X-ray diffraction data of **2**–**4** were collected using graphite-monochromated Mo-K_α radiation (λ = 0.71073 Å) with a STOE IPDS

Table 1. Crystallographic data for $^3_\infty$[Zn(S-2-$N_2C_4H_3$)$_2$] (**1**), $^2_\infty$[Cd(S-2-$N_2C_4H_3$)$_2$] (**2**), [Hg(S-2-$N_2C_4H_3$)$_2$] (**3**) and [Cd(S-2-$N_2C_4H_3$)$_2$(tmeda)] (**4**).

	1	**2**	**3**	**4**
Formula mass	287.7	334.7	422.9	450.9
Crystal system	orthorhombic	orthorhombic	monoclinic	monoclinic
Space group	$Pna2_1$	$Pbca$	$P2_1/n$	$P2_1/n$
a [Å]	7.812(2)	15.858(3)	19.300(4)	12.317(3)
b [Å]	16.526(3)	7.969(2)	3.963(1)	10.785(2)
c [Å]	7.861(2)	16.775(3)	29.367(6)	15.130(3)
β [°]	90	90	108.82(3)	109.77(3)
V [Å^3]	1014.8(4)	2119.8(7)	2126.2(7)	1891.4(7)
Z	4	8	8	14
T [K]	180	180	190	190
$D_{calcd.}$ [g cm^{-3}]	1.883	2.097	2.642	1.583
μ(Mo-K_α) [mm^{-1}]	2.798	2.422	14.839	1.382
F(000)	576	1296	1552	912
$2\theta_{max}$ [°]	51	54	54	54
Measured reflections	3895	13987	15340	9890
Unique reflections	1304	2337	4650	3993
R_{int}	0.1193	0.0624	0.09	0.0597
Reflections with $I > 2\sigma(I)$	1181	1925	3458	3365
Refined parameters	137	136	271	296
R_1 [$I > 2\sigma(I)$][a]	0.0657	0.0502	0.0441	0.0370
wR_2 (all data)[b]	0.1727	0.1539	0.1398	0.1183
Absolute structure parameter	0.54(5)	–	–	–

[a] $R_1 = \Sigma||F_o| - |F_c||/\Sigma|F_o|$. [b] $wR_2 = \{\Sigma[w(F_o^2 - F_c^2)^2]/\Sigma[w(F_o^2)^2]\}^{1/2}$.

II (Imaging Plate Diffraction System) equipped with a Schneider rotating anode. Single-crystal X-ray diffraction data of **1** were collected using synchrotron radiation (λ = 0.80 Å) with a STOE IPDS II (Imaging Plate Diffraction System) at the ANKA synchrotron source in Karlsruhe. The structures were solved with the direct-methods program SHELXS[29] of the SHELXTL PC suite of programs, and were refined with the use of the full-matrix least-squares program SHELXL (Table 1).[29] Molecular diagrams were prepared using SCHAKAL 97[30] and DIAMOND.[31] All Cd, Zn, S, N and C atoms were refined with anisotropic displacement parameters whilst H atoms were calculated in fixed positions. CCDC-266974 (**1**), -266975 (**2**), -266976 (**3**) and -266977 (**4**) contain the supplementary crystallographic data for this paper. These data can be obtained free of charge from The Cambridge Crystallographic Data Centre via www.ccdc.cam.ac.uk/data_request/cif. X-ray powder diffraction patterns (XRD) were measured with a STOE STADI P diffractometer (Cu-$K_{\alpha 1}$ radiation, germanium monochromator, Debye–Scherrer geometry) in sealed glass capillaries. A theoretical powder diffraction pattern for **1** was calculated on the basis of the atom coordinates obtained from single-crystal X-ray analysis by using the program package STOE WinXPOW.[32]

Acknowledgments

This work was supported by the Deutsch–Israelisches Programm (DIP) and the Deutsche Forschungsgemeinschaft (centre for functional nanostructures CFN). A. E. is grateful to Prof. Dr. D. Fenske for helpful discussions and for providing excellent working conditions, E. Tröster for her invaluable assistance in the practical work, Dr. E. Matern for the measurement of the ^{29}Si NMR spectra and Dr. Dale Cave for careful revision of the manuscript.

[1] E. S. Raper, *Coord. Chem. Rev.* **1996**, *153*, 199–255.
[2] E. S. Raper, *Coord. Chem. Rev.* **1997**, *165*, 475–567.
[3] M. B. Hursthouse, O. F. Z. Kahn, M. Mazid, M. Motevalli, P. O'Brien, *Polyhedron* **1990**, *9*, 541–544.
[4] M. L. Godino-Salido, M. D. Gutiérrez-Valero, R. López-Garzón, J. M. Moreno-Sánchez, *Inorg. Chim. Acta* **1994**, *221*, 177–181.
[5] R. Castro, J. A. Garcia-Vazquez, J. Romero, A. Sousa, W. Hiller, J. Strähle, *Polyhedron* **1994**, *13*, 273–279.
[6] R. Castro, J. A. Garcia-Vazquez, J. Romero, A. Sousa, R. Pritchard, C. A. McAuliffe, *J. Chem. Soc., Dalton Trans.* **1994**, 1115–1120.
[7] R. Castro, J. A. Garcia-Vazquez, J. Romero, A. Sousa, A. Castineiras, W. Hiller, J. Strähle, *Inorg. Chim. Acta* **1993**, *211*, 47–54.
[8] J. Romero, J. A. Garcia-Vazquez, A. Sousa, J. Zubieta, Y. Chang, *Polyhedron* **1996**, *15*, 2741–2745.
[9] S. Wang, J. P. Fackler, Jr., *Inorg. Chem.* **1989**, *28*, 2615–2619.
[10] A. K. Das, S. Seth, *J. Inorg. Biochem.* **1997**, *65*, 207–218.
[11] M. B. Hursthouse, O. F. Z. Kahn, M. Mazid, M. Motevalli, P. O'Brien, *Polyhedron* **1990**, *9*, 541–544.
[12] Y. Cheng, T. J. Emge, J. G. Brennan, *Inorg. Chem.* **1994**, *33*, 3711–3714.
[13] A. Eichhöfer, P. Deglmann, *Eur. J. Inorg. Chem.* **2004**, 349–355.
[14] A. Eichhöfer, O. Hampe, M. Blom, *Eur. J. Inorg. Chem.* **2003**, 1307–1314.
[15] A. Eichhöfer, A. Aharoni, U. Banin, *Z. Anorg. Allg. Chem.* **2002**, *628*, 2415–2421.
[16] V. Soloviev, A. Eichhöfer, D. Fenske, U. Banin, *J. Am. Chem. Soc.* **2001**, *123*, 2354–2364.
[17] S. Behrens, M. Bettenhausen, A. C. Deveson, A. Eichhöfer, D. Fenske, A. Lohde, U. Woggon, *Angew. Chem.* **1996**, *108*, 2360–2363; *Angew. Chem. Int. Ed. Engl.* **1996**, *35*, 2215–2218.
[18] R. Castro, M. L. Duran, J. A. Garcia-Vazquez, J. Romero, A. Sousa, A. Castineiras, W. Hiller, J. Strähle, *Z. Naturforsch. B* **1992**, *47*, 1067–1074.
[19] M. J. Nowak, H. Rostkowska, L. Lapinski, J. Leszczynski, J. S. Kwiatkowski, *Spectrochim. Acta, Part A* **1991**, *47*, 339–353.
[20] D. N. Sathyanarayana, S. V. Kasimir Raja, *Spectrochim. Acta, Part A* **1985**, *41*, 809–813.
[21] B. P. Kennedy, A. B. P. Lever, *Can. J. Chem.* **1972**, *50*, 3488–3507.
[22] S. Stoyanov, I. Petkov, L. Antonov, T. Stoyanova, *Can. J. Chem.* **1990**, *68*, 1482–1489.
[23] B. R. Penfold, *Acta Crystallogr.* **1953**, *6*, 707–713.
[24] H. T. Flakus, A. Tyl, P. G. Jones, *Spectrochim. Acta, Part A* **2002**, *58*, 299–310.
[25] G. H. Keller, L. Bauer, C. L. Bell, *Can. J. Chem.* **1968**, *46*, 2475–2479.
[26] D. A. Thornton, *Coord. Chem. Rev.* **1990**, *104*, 251–295.
[27] Y. Saito, M. Cordes, K. Nakamoto, *Spectrochim. Acta, Part A* **1972**, *28*, 1459–1466.
[28] H. Vorbrüggen, P. Strehlke, *Chem. Ber.* **1973**, *106*, 3039–3061.
[29] G. M. Sheldrick, *SHELXTL, An Integrated System for Solving, Refining, and Displaying Crystal Structures from Diffraction Data*, PC version 5.1, Bruker Analytical X-ray Systems, Karlsruhe, **2000**.
[30] E. Keller, *SCHAKAL 97, A Computer Program for the Graphic Representation of Molecular and Crystallographic Models*, University of Freiburg, **1997**.
[31] K. Brandenburg, *DIAMOND*, version 2.1d, Visual Crystal Structure Information System, Bonn, **2000**.
[32] *STOE WinXPOW*, STOE & Cie GmbH, Darmstadt, **2000**.

Received: March 23, 2005
Published Online: September 7, 2005

